ARTICLE

Determining the relative structural relevance of halogen and hydrogen bonds in self-assembled monolayers

Received 00th January 20xx,
Accepted 00th January 20xx

DOI: 10.1039/x0xx00000x

Harry Pinfold,[a] Marco Sacchi,[b] Graham Pattison[a]‡ and Giovanni Costantini [a]*

Although hydrogen bonds have long been established as a highly effective intermolecular interaction for controlling the formation of self-assembled monolayers, the potential utility of the closely related halogen bonds has only recently emerged. The cooperative use of both halogen and hydrogen bonds provides a unique, multitiered strategy towards controlling the morphology of self-assembled structures. However, the interplay between these two interactions within monolayer systems has been little studied. Here, we have systematically investigated this interplay in self-assembled monolayers formed at the solid-liquid interface, with a specific attention on determining the structural relevance of the two interactions in the formation of 2D supramolecular structures. A single molecule which can simultaneously act as both a halogen and hydrogen bond donor was paired with molecules which are effective acceptors for both of these interactions. The bimolecular networks that result from these pairings were studied using scanning tunnelling microscopy coupled with density function theory calculations. Additional measurements on similar networks formed by using structural analogues in which halogen bonding interactions are no longer possible give significant insight into the structure-determining role of these interactions. We find that in some monolayer systems the halogen bonds serve no significant structure-determining role and the assembly is dominated by hydrogen bonding; however, in other systems, effective cooperation between the two interactions is observed. This study gives clear insight into the cooperative and competitive balance between halogen and hydrogen bonds in self-assembled monolayers. This information is expected to be of considerable value for the future design of monolayer systems using both halogen and hydrogen bonds.

Introduction

One of the most significant challenges in surface-confined supramolecular chemistry is predicting the architecture of self-assembled monolayers based on the structure of the molecular building blocks from which they are constructed. The morphology of such networks is governed by both the lateral intermolecular interactions between the building blocks and the interaction between these molecules and the underlying surface. The subtle interplay between these different factors makes prediction of monolayer structure extremely challenging. One way to circumvent this issue is to utilise strong intermolecular interactions which are capable of dominating the self-assembly process. In this way, structures with more predictable morphologies can be constructed. A range of different intermolecular interactions including hydrogen bonds[1–4], van der Waals interactions[5] and metal-organic coordination[6] can be utilised in this manner.

Hydrogen bonds have been particularly widely exploited for driving the formation of self-assembled monolayers. These interactions are both strong and directional, two properties which make them ideal for controlling the formation of stable, ordered networks. Halogen bonds, the comparatively little-studied 'cousin' of the hydrogen bond, have recently emerged as an interesting addition to the toolbox of interactions used in surface-confined supramolecular chemistry. When a halogen atom is attached to an electron-withdrawing group, the electron density surrounding it can become polarised.[7] This results in the halogen atom having an electrophilic region, known as the σ-hole, centred at the antipode of the covalent bond attaching it to the electron-withdrawing group. The interaction between the electrophilic σ-hole and a nucleophilic site constitutes a halogen bond. Although they are typically somewhat weaker than hydrogen bonds, they have higher directionality[8–11]. The ability of halogen bonds to drive the formation of self-assembled monolayers has been demonstrated with a range of different molecular building blocks.[12] For example, strong I···N(pyridyl) halogen bonds have even been shown to be capable of stabilising porous networks under the thermodynamically challenging conditions present at the solid-liquid interface.[13–15]

One particularly interesting avenue for the design of supramolecular systems is the cooperative use of halogen and hydrogen bonds. By simultaneously employing these two directional interactions, it is possible to gain additional levels of control over the self-assembly process. This has been particularly widely explored in three-dimensional systems,

[a] Department of Chemistry, University of Warwick, Gibbet Hill Road, Coventry, CV4 7AL, UK. E-mail: g.costantini@warwick.ac.uk
[b] Department of Chemistry, University of Surrey, Guildford, GU2 7XH, UK.
† Electronic Supplementary Information (ESI) available: Experimental details, additional STM images and calculations. See DOI: 10.1039/x0xx00000x
‡ Present address: Chemistry Research Group, School of Pharmacy and Biomolecular Sciences, University of Brighton, Brighton, BN2 4GJ, UK.

where halogen and hydrogen bonds have been shown to be capable of synergistically controlling the formation of complex ordered structures.[16–26] It has also been demonstrated that in some instances these interactions can compete such that one dominates the self-assembly process at the expense of the other.[24–27] Within 2D supramolecular systems, some explicit efforts to probe the interplay between halogen and hydrogen bonds have been made.[28–31] However, the true structural significance of the halogen bonding interactions proposed within these studies remains particularly unclear. Typically, the formation of strong halogen bonds requires that the halogen bond donating atom is polarised via attachment to a significantly powerful electron-withdrawing group. This criterion is not fulfilled in the current literature on the balance between halogen and hydrogen bonds in 2D systems. Furthermore, most of the molecular building blocks used within these studies contain long alkyl chains.[29–31] Alkyl chain interdigitation is known to have a significant impact on the morphology of self-assembled monolayers,[5] and this dominant influence could thus mask the true structural significance of the proposed halogen/hydrogen bonds.

In this contribution, we have used scanning tunnelling microscopy (STM) coupled with density functional theory (DFT) to study a series of self-assembled monolayers formed at the solid–liquid interface. These monolayers are constructed using multifunctional molecular building blocks which can interact via both halogen and hydrogen bonds. By studying analogous systems in which halogen bonds are no longer possible, we are able to probe the structure-controlling influence of these interactions. We demonstrate that in some systems the halogen and hydrogen bonds compete, whereas in others these interactions function cooperatively to govern the morphology of the resultant supramolecular structure. This unique approach gives a significant and so-far missing insight into the balance between hydrogen and halogen bonding interactions in self-assembled monolayers.

Results and discussion

The structures of the molecular building blocks used within this study are shown in Fig. 1. We strictly avoided using molecules containing alkyl chains as the dominant effect these can have in controlling the morphology of self-assembled monolayers may obscure the influence of the interactions of interest. 4BTFBA is a planar aromatic molecule functionalised with a bromine atom and a carboxyl group. These two substituents are positioned para to one another. 4BTFBA can act as a halogen bond donor via its bromine atom and a hydrogen bond donor via its carboxyl group. The aromatic core is fluorinated as the electron-withdrawing influence of the fluorine atoms is expected to significantly increase the halogen bond donor ability of the bromine atom.[7] 3TPTZ and 4TPTZ were employed as potential acceptors for both halogen and hydrogen bonds. These two planar molecules are structural isomers differing in the positions of their pyridyl nitrogen atoms. The nitrogen atoms within such pyridyl groups have previously been shown to be effective halogen bond acceptor sites in networks formed under

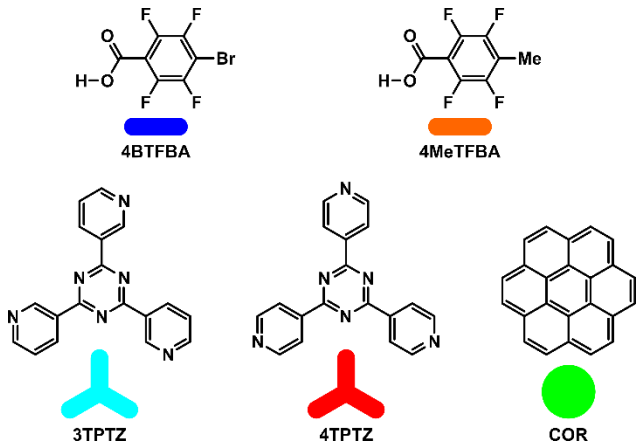

Fig. 1 Structures of the molecular building blocks used in this study: 4-bromo-2,3,5,6-tetrafluorobenzoic acid (4BTFBA), 4-methyl-2,3,5,6-tetrafluorobenzoic acid (4MeTFBA), 2,4,6-tri(3-pyridyl)-s-triazine (3TPTZ), 2,4,6-tri(4-pyridyl)-s-triazine (4TPTZ) and coronene (COR). The coloured shapes are schematic representations of the building blocks.

similar conditions to those used in this study.[13–15] Furthermore, we have previously demonstrated that 3TPTZ and 4TPTZ interact very favourably with fluorinated carboxylic acids, like 4BTFBA, via strong O–H···N(pyridyl) interactions.[32] 4MeTFBA was employed as a structural analogue of 4BTFBA. In 4MeTFBA a methyl group is present at the location of the bromine atom in 4BTFBA. This structural analogue was selected since it is expected to have essentially the same dimensions as 4BTFBA, given that the vdW radius of the methyl group (2.0 Å[33]) closely matches that of a single bromine atom (1.85 Å[34]). The two analogues should be able to partake in all the same intermolecular interactions other than any halogen bonds, which are clearly not possible with 4MeTFBA (see ESI† section 3). Furthermore, the presence of the methyl group is not expected to introduce the potential for any additional strong intermolecular interactions. The minimal steric impact associated with exchanging bromine atoms and methyl groups has previously been used in a biochemical setting, where bioisosteric exchange of bromo and methyl groups can give insight into ligand-protein interactions.[35,36] Similarly, the ease of incorporation of 5-bromouracil into DNA in place of thymine (5-methyluracil) is thought to be a result of the comparable dimensions of the two molecules.[37] Here, we use exchange of 4BTFBA for 4MeTFBA to gain insight into the structural significance of any halogen bonding interactions which appear to be present in systems containing 4BTFBA. Finally, coronene was employed as a guest molecule. As is shown in the following, many of the networks we observe are porous and the incorporation of coronene into these pores gives significant insight into the nature of the assembly. Our methodology was as follows: (i) codeposit 4BTFBA with 4TPTZ/3TPTZ and examine the resultant networks via STM and DFT; (ii) if halogen bonding interactions appear to be present, study the analogous systems in which 4BTFBA has been exchanged for 4MeTFBA; (iii) if isostructural networks can be formed using both 4BTFBA and 4MeTFBA, halogen bonds are not considered to be structurally significant.

Competition Between Halogen and Hydrogen Bonds

First, we investigated the coassembly of 4BTFBA with 4TPTZ. Deposition of a solution containing these two molecules leads to the formation of an ordered monolayer at the 1-phenyloctane/HOPG interface. Extended domains of this network could be readily observed via STM (see Fig. S21). The assembly is approximately hexagonal, having two equivalent lattice vectors with lengths of 2.9 ± 0.2 nm separated by an angle of 60 ± 3°. Fig. 2a shows a high-resolution STM image of the assembly in which the threefold-symmetric 4TPTZ molecules and the rodlike 4BTFBA molecules can be clearly resolved. The 4BTFBA molecules are positioned such that they can interact with the pyridyl nitrogen atoms of the 4TPTZ molecules. However, their relative orientation cannot be identified from the STM images, hence it is unclear if their bromine atoms or their carboxyl groups are orientated towards the pyridyl nitrogen atoms. This issue will be addressed later on. The network of 4BTFBA and 4TPTZ molecules defines a series 'pores' which appear to be occupied. The occupants have a 'streaky' appearance consistent with the presence of molecular motion. We expect that these mobile species are either solvent molecules or 4BTFBA molecules as the pores are too small to reasonably accommodate 4TPTZ molecules. Further insight into the assembly was obtained by exploring its ability to act as a host network for coronene guest molecules. As is shown in Fig. 2b, the mobile pore occupants could be readily displaced by coronene molecules without perturbation to the unit cell dimensions of the network. The ability of this network to partake in host–guest chemistry hints at the robustness of the assembly. We expect that these pores are highly effective guest sites for coronene as the hydrogen atoms on the periphery of the coronene molecules can interact with the fluorine atoms lining the interior of the pores via favourable C–H···F interactions.

In order to obtain a detailed structural model and to determine the orientation of the 4BTFBA molecules, DFT calculations were employed. As previously mentioned, the 4BTFBA molecules are positioned such that they can either hydrogen bond to the N(pyridyl) atoms of the 4TPTZ molecules via their carboxyl groups or halogen bond to the same atoms via their bromine atoms. When the surface-induced chirality of the 4BTFBA molecules is considered, there are four possible distinct configurations that are compatible with the STM data (see Fig. S7). The four potential configurations were all optimised via DFT. The lowest energy configuration, and therefore the one which we expect is present in the assembly, is shown in Fig. 3. The unit cell dimensions of this optimised model closely match those observed experimentally. The species adsorbed within the pores were not included in the calculations due to their mobility. However, the intrapore species' mobility and the fact that they can be readily displaced by coronene molecules indicates that their interaction with the surrounding network is minimal and that their presence likely has little impact on its structure. Within the optimised model, the carboxyl groups of the 4BTFBA molecules are orientated towards the 4TPTZ molecules such that they can interact with them via strong O–H···N(pyridyl) hydrogen bonds. The bromine atoms of the 4BTFBA molecules are positioned such that they can halogen bond to neighbouring 4BTFBA molecules via Br···O interactions. Within the optimised model, the Br···O separation (d in Fig. 3b) is 2.82 ± 0.01 Å (see section 5 of the ESI† for the definition of this theoretical value and uncertainty), which is significantly smaller than the sum of the vdW radii for bromine and oxygen (3.37 Å[34]). Additionally, the C–Br···O angle (θ in Fig. 3b) of 168 ± 1° is close to the linear geometry expected for halogen bonding interactions. The small separation and close-to-linear angle both indicate that Br···O halogen bonds are present.[38] It should be noted that the 4BTFBA molecules are not orientated such that the halogen bonds can occur along the projection of one of the partaking carbonyl oxygen atoms' lone pairs. However, although such alignment is optimal, interactions of appreciable strength can be observed without this.[7] C–H···F interactions, which have been shown to be significant in other 2D systems,[39–43] also likely contribute towards stabilising the assembly. Furthermore, there may also be an auxiliary contribution form weak C–H···O interactions.

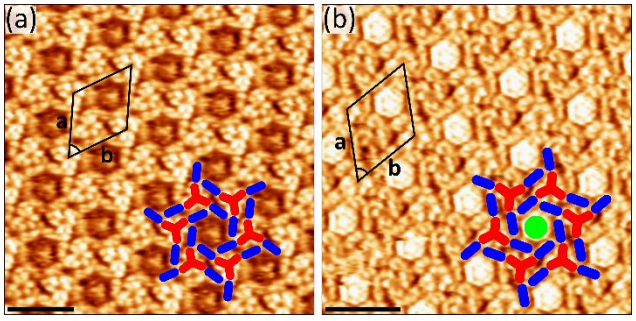

Fig. 2 STM images showing the coassembly of 4BTFBA and 4TPTZ at the 1-phenyloctane/HOPG interface (a) without coronene inclusion and (b) with coronene inclusion. The schematic representations given in Fig. 1 are overlaid onto the STM images to highlight the relative positions of the molecules. Unit cell parameters: a = b = 2.9 ± 0.2 nm, angle = 60 ± 3°. Tunnelling conditions: (a) V_{bias} = −1200 mV, I_{set} = 300 pA, (b) V_{bias} = −1200 mV, I_{set} = 300 pA. Both scale bars = 3 nm.

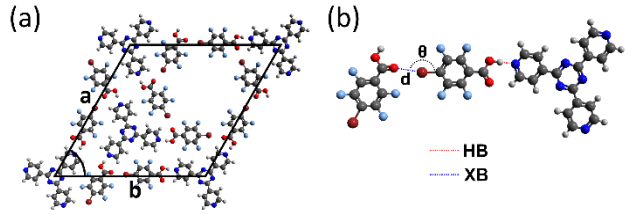

Fig. 3 (a) DFT optimised model for the coassembly of 4BTFBA and 4TPTZ. Unit cell parameters: a = b = 2.81 nm, angle = 60.4°. (b) Schematic highlighting the significant distances and angles associated with the Br···O halogen bonds.

Although both halogen and hydrogen bonds seem to be present within the assembly, the relative structural significance of these interactions remains unclear. In order to evaluate this, we studied analogous systems in which 4BTFBA was exchanged for 4MeTFBA. 4MeTFBA was also observed to coassemble with 4TPTZ into a hexagonal network at the 1-phenyloctane/HOPG interface. Note that a range of other structures could also be formed based on the solution composition (see ESI† section 6). The lattice parameters of the hexagonal assembly are identical to those of the network formed between 4BTFBA and 4TPTZ.

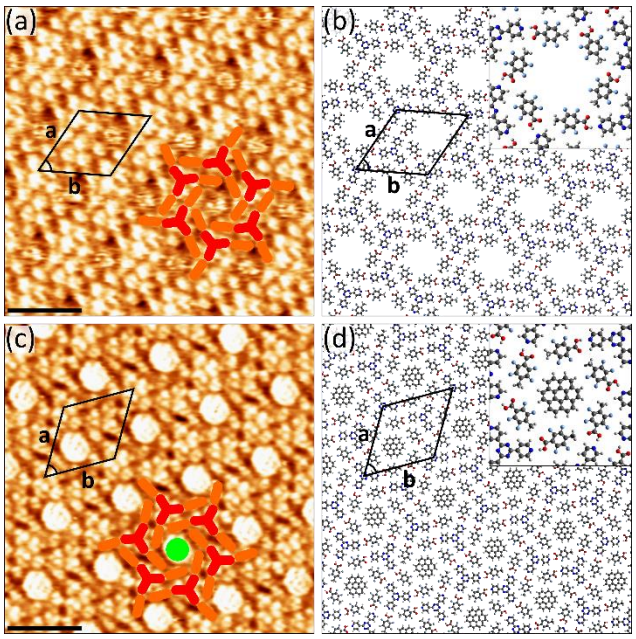

Fig. 4 STM images showing the coassembly of 4MeTFBA and 4TPTZ at the 1-phenyloctane/HOPG interface (a) without coronene inclusion and (c) with coronene inclusion. The schematic representations given in Fig. 1 are overlaid onto the STM images to highlight the relative positions of the molecules. The proposed models for the assembly are shown (b) without coronene inclusion and (d) with coronene inclusion. Unit cell parameters: a = b = 2.9 ± 0.2 nm, angle = 60 ± 3°. Tunnelling conditions: (a) V_{bias} = −1200 mV, I_{set} = 300 pA, (b) V_{bias} = −1200 mV, I_{set} = 300 pA. Both scale bars = 3 nm.

Fig. 4a shows a high-resolution STM image of the hexagonal assembly. From such images, it becomes clear that this network is isostructural with that formed between 4BTFBA and 4TPTZ. The 4MeTFBA molecules are again able to partake in the same O–H···N(pyridyl), C–H···F and C–H···O interactions as the 4BTFBA molecules, but Br···O halogen bonds are no longer possible. The fact that the same network can be sustained in the absence of the Br···O interactions demonstrates that these interactions have little influence on the morphology of the 4BTFBA/4TPTZ network. Mobile species are also present within the pores of the hexagonal 4MeTFBA/4TPTZ network, and these can again be readily displaced by coronene guest molecules (see Fig. 4c). The fact that the hexagonal 4MeTFBA/4TPTZ assembly is also robust enough to partake in host-guest chemistry further undermines the significance of the Br···O halogen bonds seemingly present in the 4BTFBA/4TPTZ system.

In principle, the N(pyridyl) atoms of the 4TPTZ molecules should be superior halogen bond acceptor sites to the carbonyl oxygen atoms of 4BTFBA, as has been shown in a range of different systems.[44–50] This effect is also consistent with the electrostatic potential energy surfaces for 4BTFBA and 4TPTZ (see ESI† section 3), where the magnitude of the negative electrostatic potential energy associated with N(pyridyl) atoms of 4TPTZ is greater than the corresponding value for the carbonyl oxygen atom of 4BTFBA. However, within the coassembly of 4BTFBA with 4TPZ, the formation of Br···N(pyridyl) halogen bonds is not observed. Rather, the pyridyl nitrogen atoms of the 4TPTZ molecules interact with the carboxyl groups of the 4BTFBA molecules via O–H···N(pyridyl) interactions. Although the N(pyridyl) sites would be the optimal available halogen bond acceptor sites, they are also expected to be the optimal available sites with which the carboxyl group of the 4BTFBA molecules can interact via hydrogen bonds.[51–54] The proclivity that both the carboxyl groups and bromine atoms have for interacting with N(pyridyl) sites places these two interactions in direct competition. Evidently, the carboxyl groups win this competition, with O–H···N(pyridyl) hydrogen bonds being formed in preference to Br···N(pyridyl) halogen bonds. The bromine atoms of the 4BTFBA molecules are seemingly relegated to the inferior carbonyl oxygen acceptor sites, and they are accordingly positioned such that they can partake in these secondary Br···O halogen bonds; however, as the results with 4MeTFBA demonstrate, these interactions are of very limited structural significance. Although these Br···O halogen bonds may have some stabilising influence, the isostructurality observed with 4MeTFBA suggests their presence may in fact be a simple consequence of the packing of the assembly, which is mediated by other intermolecular interactions and the interaction between the molecules and the surface, rather than there being any particular driving force for their formation.

Cooperation Between Halogen and Hydrogen Bonds

3TPTZ and 4BTFBA also coassemble into a bimolecular network at the 1-phenyloctane/HOPG interface (see Fig. S23). This approximately hexagonal assembly has two identical lattice vectors with lengths of 3.2 ± 0.3 nm, separated by an angle of 60 ± 3°. High resolution STM images, such as that presented in Fig. 5a, can be used to partially elucidate the structure of the assembly. As is highlighted by the overlay shown in Fig. 5a, the 3TPTZ and 4BTFBA molecules can both be resolved. The hexagonal 4BTFBA/3TPTZ system possesses many similarities with the 4BTFBA/4TPTZ system. The 4BTFBA molecules are similarly positioned such that they can interact with the pyridyl nitrogen atoms of the 3TPTZ molecules, but again the precise orientation of the 4BTFBA molecules cannot be obtained from the STM images alone. The 4BTFBA molecules are arranged such that they define a series of hexagonal pores which appear

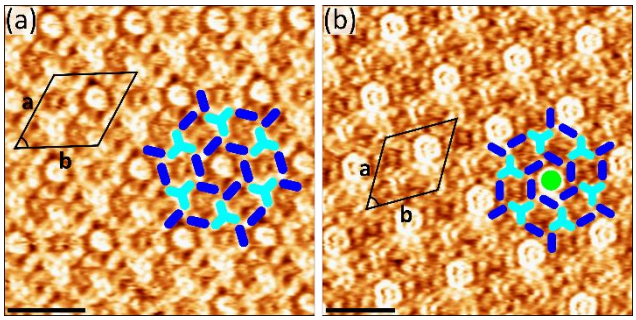

Fig. 5 STM images showing the coassembly of 4BTFBA and 3TPTZ at the 1-phenyloctane/HOPG interface (a) without coronene inclusion and (b) with coronene inclusion. The schematic representations given in Fig. 1 are overlaid onto the STM images to highlight the relative positions of the molecules. Unit cell parameters: a = b = 3.2 ± 0.3 nm, angle = 60 ± 3°. Tunnelling conditions: (a) V_{bias} = −1200 mV, I_{set} = 70 pA, (b) V_{bias} = −1200 mV, I_{set} = 100 pA. Both scale bars = 3 nm.

to be very similar to the pores present in the 4BTFBA/4TPTZ system. Again, these pores are occupied by a seemingly mobile species – very clearly resolved in Fig. 5a – that could again be readily displaced by coronene guest molecules without altering the unit cell dimensions of the host network (see Fig. 5b). The main difference between the two assemblies is that the angle at which the 4BTFBA interact with the 3TPTZ molecules is shifted due to the different position of the N(pyridyl) atoms in 3TPTZ when compared with 4TPTZ. This results in the 4BTFBA/3TPTZ assembly being relatively more porous than the 4BTFBA/4TPTZ system: in addition to the main hexagonal pores which can host coronene guest molecules, additional smaller pores are also present. It is unclear if the smaller pores are occupied or not; however, these pores appear to be too small to reasonably accommodate any of the molecular species present in a planar configuration, hence any interactions between possible adsorbed species and the surrounding network are expected to be relatively weak.

DFT calculations were employed in the same manner as those that were used for the 4BTFBA/4TPTZ system, i.e., by optimising the four possible configurations that are compatible with the STM data (Fig. S8). Of the four possible configurations, the structure in which the 4BTFBA molecules are arranged into the same hexagonal motif present in the 4BTFBA/4TPTZ system was also found to be favoured in this case. Within the optimised structure (see Fig. 6), each 4BTFBA molecule is positioned such that it can form a strong O–H···N(pyridyl) hydrogen bond with an adjacent 3TPTZ molecule. The bromine atoms are again positioned such that each can halogen bond to the carbonyl oxygen of a neighbouring 4BTFBA molecule via a Br···O interaction. In the optimised model, the Br···O separation (d in Fig. 6b) is 2.85 ± 0.03 Å and the C–Br···O angle (θ in Fig. 6b) is 174.3 ± 0.3°. The close-to-linear angle and interatomic separation which is much smaller than the sum of the vdW radii of oxygen and bromine (3.37 Å[34]) indicate that Br···O halogen bonds are present. Substitution of 4BTFBA for 4MeTFBA was again explored in an effort to probe the structural significance of the proposed Br···O halogen bonds. Although 4MeTFBA and 3TPTZ were observed to cossemble into a range of different structures (see ESI† section 6), none of these networks is isostructural with the hexagonal assembly of 4BTFBA and 3TPTZ. This hints that the Br···O halogen bonds may be of structural significance here.

Overall, the interplay between halogen and hydrogen bonds in the hexagonal 4BTFBA/3TPTZ system appears to be influenced by a balance between competitive and cooperative

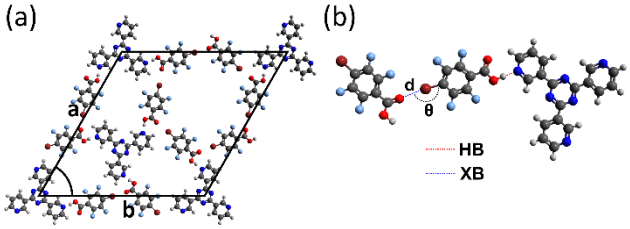

Fig. 6 (a) DFT optimised model for the hexagonal coassembly of 4BTFBA and 3TPTZ. Unit cell parameters: a = b = 3.09 nm, angle = 60.1°. (b) Schematic highlighting the significant distances and angles associated with the potential Br···O halogen bonds.

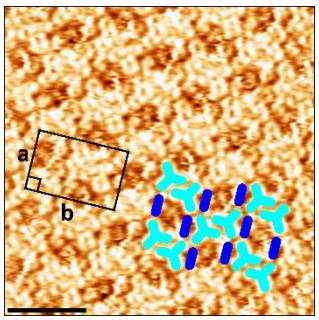

Fig. 7 STM image showing the rectangular coassembly of 4BTFBA and 3TPTZ at the 1-phenyloctane/HOPG interface. The schematic representations given in Fig. 1 are overlaid onto the STM image to highlight the relative positions of the molecules. Unit cell parameters: a = 2.3 ± 0.2 nm, b = 3.5 ± 0.3 nm, angle = 90 ± 3°. Tunnelling conditions: V_{bias} = −1200 mV, I_{set} = 300 pA, Scale bar = 3 nm.

effects. As was the case in the coassembly of 4BTFBA with 4TPTZ, within the hexagonal 4BTFBA/3TPTZ system, the carboxyl groups of the 4BTFBA molecules outcompete their bromine atoms for the optimal N(pyridyl) acceptor sites, with the preferential formation of O–H···N(pyridyl) hydrogen bonds over Br···N(pyridyl) halogen bonds again being observed. The bromine atoms of the 4BTFBA molecules are also similarly positioned such that they can interact with neighbouring 4BTFBA molecules via Br···O halogen bonds; however, unlike in the 4BTFBA/4TPTZ system, these Br···O halogen bonds seem to have a more prominent structural role in the hexagonal 4BTFBA/3TPTZ system. This is evidenced by the fact that isostructural networks could not be constructed when 4BTFBA was exchanged for 4MeTFBA. In this case, the strong O–H···N(pyridyl) hydrogen bonds, which clearly play a significant structural role, cooperate with the weaker Br···O halogen bond to help control the organisation of the molecules within the assembly. However, as is discussed below, the hexagonal assembly was only observed to be metastable. Although this system does seem to be consistent with one cooperatively stabilised by both halogen and hydrogen bonds, these interactions are not sufficient to render the assembly thermodynamically stable.

The hexagonal assembly of 3TPTZ and 4BTFBA was typically stable for several hours, after which time it was observed to convert to an alternate rectangular network. It should be noted that this transformation was never observed when coronene guest molecules were adsorbed in the pores of the hexagonal assembly, suggesting that their presence stabilises the network. The rectangular network could also be directly formed, i.e., without the preceding hexagonal network, by using a relatively lower concentration of 4BTFBA in solution (see ESI† section 1). The rectangular assembly has two inequivalent lattice vectors, with lengths of 3.5 ± 0.3 nm and 2.3 ± 0.2 nm, separated by an angle of 90 ± 3°. It should be noted that this unit cell is only valid locally as the assembly is characterised by a high number of defects (see ESI† section 9). A high-resolution STM image of the rectangular network is shown in Fig. 7. The assembly in this case differs markedly from either of the hexagonal networks described above. The 4BTFBA molecules are each positioned such that they can bridge two 3TPTZ molecules by interacting with their N(pyridyl) atoms via their carboxyl groups at one end

and their bromine atoms at the other. Note that for this to happen, one of the pyridyl rings within each 3TPTZ molecule must be flipped such that the 3TPTZ molecules adopt a non-threefold symmetric conformation (see ESI† section 7). This conformation differs from that of the 3TPTZ molecules in the hexagonal 4BTFBA/3TPTZ system. Only two of the N(pyridyl) atoms in each 3TPTZ molecule are positioned such that they can interact with the 4BTFBA molecules. The remaining N(pyridyl) atoms are positioned such that they can interact with neighbouring 3TPTZ molecules via C–H···N(pyridyl) interactions. Although weak, such interactions have been shown to be important in other 2D systems[14,55–57]. There is also likely a stabilising contribution from C–H···F and C–H···O interactions between the 4BTFBA molecules and neighbouring 3TPTZ molecules.

The two N(pyridyl) sites with which each 4BTFBA molecule appears to interact are inequivalent, and the precise orientation of the 4BTFBA molecules cannot be resolved via STM, thereforeDFT calculations were again employed in order to obtain a detailed structural model. The lowest energy configuration of the four possible alternatives (see Fig. S9) is shown in Fig. 8. The unit cell parameters for this optimised structure closely match those determined experimentally. Each 4BTFBA molecule is clearly positioned such that it can bridge two 3TPTZ molecules via an O–H···N(pyridyl) hydrogen bond at one end and a Br···N(pyridyl) halogen bond at the other. The Br···N(pyridyl) separation (d in Fig. 8b) within the optimised model is 3.07 ± 0.02 Å. This distance is significantly smaller than the sum of the van der Waals radii for bromine and nitrogen (3.4 Å[34]). This, coupled with the observation that the C–Br···N(pyridyl) angle has a close-to-linear value of 168.7 ± 0.1°, clearly indicates that Br···N(pyridyl) halogen bonds are present.

In order to gauge the structural significance of the Br···N(pyridyl) halogen bonds present in the rectangular network of 4BTFBA and 3TPTZ, 4BTFBA was again exchanged for 4MeTFBA. Although an array of different bimolecular structures could be formed via the codeposition of 4MeTFBA with 3TPTZ, none of these structures is isostructural with the rectangular network of 4BTFBA and 3TPTZ. Of particular note are the two structures shown in Fig. S18 and Fig. S19. These two bimolecular assemblies of 4MeTFBA and 3TPTZ have the same ratio of the two components as the rectangular assembly of 4BTFBA and 3TPTZ, i.e., 1:1. Additionally, they both seem to be sustained by

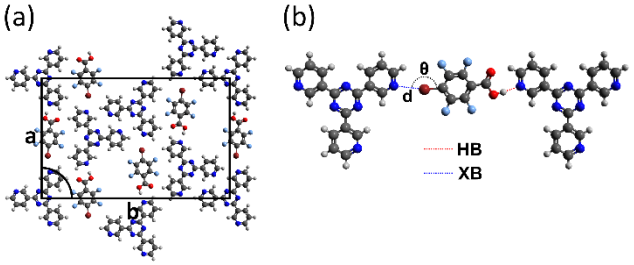

Fig. 1 (a) DFT optimised model for the rectangular coassembly of 4BTFBA and 4TPTZ. Unit cell parameters: a = 2.23 nm, b = 3.50 nm, angle = 90.1°. (b) Schematic highlighting the significant distances and angles associated with the potential Br···N(pyridyl) halogen bonds.

combinations of C–H···N(pyridyl), C–H···F, C–H···O and O–H···N(pyridyl) interactions, i.e., all the interactions that appear to be present in the rectangular coassembly of 4BTFBA and 3TPTZ other than the Br···N(pyridyl) halogen bonds. This clearly indicates that the that Br···N(pyridyl) halogen bonds play an essential structural role in the rectangular coassembly of 4BTFBA and 3TPTZ.

The interplay between halogen and hydrogen bonds within the rectangular coassembly of 4BTFBA and 3TPTZ differs markedly from that observed in the previously discussed systems. Within the rectangular network, the 4BTFBA molecules do not interact with the N(pyridyl) sites exclusively via their carboxyl groups. Instead, each simultaneously interacts with two N(pyridyl) sites via both its carboxyl group and bromine atom. Neither the carboxyl groups nor the bromine atoms completely outcompete the other for the optimal N(pyridyl) acceptor sites, with O–H···N(pyridyl) hydrogen bonds and Br···N(pyridyl) halogen bonds being formed in equal amounts. Intuitively, the strong Br···N(pyridyl) halogen bonds should be expected to play a significant structural role within the assembly. This is evidenced by the fact that isostructural networks cannot be formed upon exchanging 4BTFBA with 4MeTFBA. The rectangular coassembly of 4BTFBA and 3TPTZ represents a clear case where halogen and hydrogen bonds cooperatively control the organisation of the molecules in the assembly. It should be noted that, although halogen and hydrogen bonds are both significant, there are a range of other secondary intermolecular interactions at play which likely also exert some structure controlling influence. Furthermore, the influence of the surface also cannot be neglected. The rectangular network of 4BTFBA and 3TPTZ appears to be quite densely packed, particularly when compared to its hexagonal counterpart. This dense packing, which increases the favourable adsorption energy per unit area, may also be a particularly significant factor in determining the organisation of the molecules within the rectangular assembly.

Conclusions

The cooperative use of both halogen and hydrogen bonds clearly represents an interesting strategy for controlling the morphology of self-assembled monolayers. However, the precise balance between these interactions remains difficult to understand. As expected, strong O–H···N(pyridyl) hydrogen bonding interactions clearly play a significant structural role in all of the monolayer systems described within this text. Conversely, the precise structural role of halogen bonding interactions is much less clear-cut and challenging to predict. Whilst halogen bonds appear to play no structure-determining role in the coassembly of 4BTFBA with 4TPTZ, they are of clear significance in the coassembly of 4BTFBA with 3TPTZ.

Furthermore, our results highlight the care that must be taken when determining the structural significance of apparent intermolecular interactions within self-assembled monolayers. Within STM studies, intermolecular interactions are often assigned simply based on the relative positions and orientations of neighbouring molecules. However, this does not guarantee

that they are of any meaningful structural significance. This is clearly highlighted by the isostructurality observed between the 4BTFBA/4TPTZ and 4MeTFBA/4TPTZ systems. The use of structural analogues in the manner that we have done here provides a rational approach which can give insight into the true significance of specific intermolecular interactions.

As mentioned, the structural role of the halogen bonding interactions within these systems suffers from limited predictability. Although the bromine atoms in 4BTFBA have been activated towards halogen bonding via fluorination of the aromatic core, these interactions are still expected to be significantly weaker than the consistently observed O–H···N(pyridyl) hydrogen bonds. The use of stronger halogen bond donating groups may allow the halogen bonds to serve a more predictable structural role. Future studies will focus on determining how the interplay between halogen and hydrogen bonds is influenced by the strength of the halogen bond donor site. The methodology outlined here will provide a strong foundation for such studies. Furthermore, the insight offered by this study will be of significant interest when designing monolayer systems constructed from building blocks that can interact via both hydrogen and halogen bonds.

Conflicts of interest

There are no conflicts to declare.

Acknowledgements

MS acknowledges the Royal Society for personal support through University Research Fellowship R191029.

Notes and references

1 A. G. Slater, L. M. A. Perdigão, P. H. Beton and N. R. Champness, *Acc. Chem. Res.*, 2014, **47**, 3417–3427.
2 S. De Feyter and F. C. De Schryver, *Chem. Soc. Rev.*, 2003, **32**, 139–150.
3 O. Ivasenko and D. F. Perepichka, *Chem. Soc. Rev.*, 2011, **40**, 191–206.
4 M. Lackinger and W. M. Heckl, *Langmuir*, 2009, **25**, 11307–11321.
5 K. Tahara, S. Lei, J. Adisoejoso, S. De Feyter and Y. Tobe, *Chem. Commun.*, 2010, **46**, 8507–8525.
6 L. Dong, Z. Gao and N. Lin, *Prog. Surf. Sci.*, 2016, **91**, 101–135.
7 K. E. Riley, J. S. Murray, J. Fanfrlík, J. Řezáč, R. J. Solá, M. C. Concha, F. M. Ramos and P. Politzer, *J. Mol. Model.*, 2011, **17**, 3309–3318.
8 P. Politzer, J. S. Murray and T. Clark, *Phys. Chem. Chem. Phys.*, 2010, **12**, 7748–7757.
9 A. C. Legon, *Phys. Chem. Chem. Phys.*, 2010, **12**, 7736–7747.
10 A. C. Legon, *Angew. Chem. Int. Ed.*, 1999, **38**, 2686–2714.
11 Y.-Z. Zheng, G. Deng, Y. Zhou, H.-Y. Sun and Z.-W. Yu, *ChemPhysChem*, 2015, **16**, 2594–2601.
12 J. Teyssandier, K. S. Mali and S. De Feyter, *ChemistryOpen*, 2020, **9**, 225–241.
13 Q.-N. Zheng, X.-H. Liu, T. Chen, H.-J. Yan, T. Cook, D. Wang, P. J. Stang and L.-J. Wan, *J. Am. Chem. Soc.*, 2015, **137**, 6128–6131.
14 A. Mukherjee, J. Teyssandier, G. Hennrich, S. De Feyter and K. S. Mali, *Chem. Sci.*, 2017, **8**, 3759–3769.
15 Y. Kikkawa, M. Nagasaki, E. Koyama, S. Tsuzuki and K. Hiratani, *Chem. Commun.*, 2019, **55**, 3955–3958.
16 B. K. Saha, A. Nangia and M. Jaskólski, *CrystEngComm*, 2005, **7**, 355–358.
17 S. Tothadi and G. R. Desiraju, *Chem. Commun.*, 2013, **49**, 7791–7793.
18 C. B. Aakeröy, J. Desper, B. A. Helfrich, P. Metrangolo, T. Pilati, G. Resnati and A. Stevenazzi, *Chem. Commun.*, 2007, 4236–4238.
19 C. B. Aakeröy, P. D. Chopade, C. Ganser and J. Desper, *Chem. Commun.*, 2011, **47**, 4688–4690.
20 C. B. Aakeröy, P. D. Chopade and J. Desper, *Cryst. Growth Des.*, 2011, **11**, 5333–5336.
21 C. B. Aakeröy, N. C. Schultheiss, A. Rajbanshi, J. Desper and C. Moore, *Cryst. Growth Des.*, 2009, **9**, 432–441.
22 S. Zhu, C. Xing, W. Xu, G. Jin and Z. Li, *Cryst. Growth Des.*, 2004, **4**, 53–56.
23 B. A. DeHaven, A. L. Chen, E. A. Shimizu, S. R. Salpage, M. D. Smith and L. S. Shimizu, *Supramol. Chem.*, 2018, **30**, 315–327.
24 C. B. Aakeröy, M. Fasulo, N. Schultheiss, J. Desper and C. Moore, *J. Am. Chem. Soc.*, 2007, **129**, 13772–13773.
25 C. B. Aakeröy, S. Panikkattu, P. D. Chopade and J. Desper, *CrystEngComm*, 2013, **15**, 3125–3136.
26 C. B. Aakeröy, C. L. Spartz, S. Dembowski, S. Dwyre and J. Desper, *IUCrJ*, 2015, **2**, 498–510.
27 E. Corradi, S. V. Meille, M. T. Messina, P. Metrangolo and G. Resnati, *Angew. Chem. Int. Ed.*, 2000, **39**, 1782–1786.
28 S. Yasuda, A. Furuya and K. Murakoshi, *RSC Adv.*, 2014, **4**, 58567–58572.
29 Y. Wu, J. Li, Y. Yuan, M. Dong, B. Zha, X. Miao, Y. Hu and W. Deng, *Phys. Chem. Chem. Phys.*, 2017, **19**, 3143–3150.
30 B. Zha, J. Li, J. Wu, X. Miao and M. Zhang, *New J. Chem.*, 2019, **43**, 17182–17187.
31 M. Dong, T. Hu, Y. Wang, P. Pang, Y. Wang, X. Miao, B. Li and W. Deng, *Appl. Surf. Sci.*, 2020, **515**, 145983.
32 H. Pinfold, C. Greenland, G. Pattison and G. Costantini, *Chem. Commun.*, 2020, **56**, 125–128.
33 L. Pauling, *The Nature of the Chemical Bond*, Cornell University Press, Ithaca, New York, 3rd edn., 1960. pp.261.
34 A. Bondi, *J. Phys. Chem.*, 1964, **68**, 441–451.
35 E. E. Carlson, J. F. May and L. L. Kiessling, *Chem. Biol.*, 2006, **13**, 825–837.
36 S. Park, K. L. Morley, G. P. Horsman, M. Holmquist, K. Hult and R. J. Kazlauskas, *Chem. Biol.*, 2005, **12**, 45–54.
37 S. Zamenhof, B. Reiner, R. D. Giovanni and K. Rich, *J. Biol. Chem.*, 1956, **219**, 165–173.
38 G. R. Desiraju, P. S. Ho, L. Kloo, A. C. Legon, R. Marquardt, P. Metrangolo, P. Politzer, G. Resnati and K. Rissanen, *Pure Appl. Chem.*, 2013, **85**, 1711–1713.
39 A. Y. Brewer, M. Sacchi, J. E. Parker, C. L. Truscott, S. J. Jenkins and S. M. Clarke, *Phys. Chem. Chem. Phys.*, 2014, **16**, 19608–19617.
40 J. Niederhausen, Y. Zhang, F. Cheenicode Kabeer, Y. Garmshausen, B. M. Schmidt, Y. Li, K.-F. Braun, S. Hecht, A. Tkatchenko, N. Koch and S.-W. Hla, *J. Phys. Chem. C*, 2018, **122**, 18902–18911.
41 Z. Mu, L. Shu, H. Fuchs, M. Mayor and L. Chi, *J. Am. Chem. Soc.*, 2008, **130**, 10840–10841.
42 V. Oison, M. Koudia, M. Abel and L. Porte, *Phys. Rev. B*, 2007, **75**, 035428.
43 E. Barrena, D. G. de Oteyza, H. Dosch and Y. Wakayama, *ChemPhysChem*, 2007, **8**, 1915–1918.
44 P. Metrangolo, W. Panzeri, F. Recupero and G. Resnati, *J. Fluorine Chem.*, 2002, **114**, 27–33.
45 J. Řezáč and A. de la Lande, *Phys. Chem. Chem. Phys.*, 2017, **19**, 791–803.

46 J. F. Bertrán and M. Rodríguez, *Org. Magn. Reson.*, 1979, **12**, 92–94.
47 D. E. Martire, J. P. Sheridan, J. W. King and S. E. O'Donnell, *J. Am. Chem. Soc.*, 1976, **98**, 3101–3106.
48 J.-Y. L. Questel, C. Laurence and J. Graton, *CrystEngComm*, 2013, **15**, 3212–3221.
49 C. Perkins, S. Libri, H. Adams and L. Brammer, *CrystEngComm*, 2012, **14**, 3033–3038.
50 M. Erdélyi, *Chem. Soc. Rev.*, 2012, **41**, 3547–3557.
51 T. R. Shattock, K. K. Arora, P. Vishweshwar and M. J. Zaworotko, *Cryst. Growth Des.*, 2008, **8**, 4533–4545.
52 T. Li, P. Zhou and A. Mattei, *CrystEngComm*, 2011, **13**, 6356–6360.
53 C. B. Aakeröy, A. M. Beatty and B. A. Helfrich, *Angew. Chem. Int. Ed.*, 2001, **113**, 3340–3342.
54 T. Steiner, *Acta Crystallogr. B*, 2001, **57**, 103–106.
55 A. Ciesielski, P. J. Szabelski, W. Rżysko, A. Cadeddu, T. R. Cook, P. J. Stang and P. Samorì, *J. Am. Chem. Soc.*, 2013, **135**, 6942–6950.
56 U. Ziener, J.-M. Lehn, A. Mourran and M. Möller, *Chem. Eur. J*, 2002, **8**, 951–957.
57 J. Zhang, B. Li, X. Cui, B. Wang, J. Yang and J. G. Hou, *J. Am. Chem. Soc.*, 2009, **131**, 5885–5890.